P-ISSN 2586-9000
E-ISSN 2586-9027
Homepage : https://tci-thaijo.org/index.php/SciTechAsia
Science & Technology Asia
Vol.26 No.3 July - September 2021
Page: [99-113]
Original research article

Leaf Age-related Acclimation in the Photosynthetic Capacity and Fractional Investments of Leaf Nitrogen in Grapevines of Different Ages

Rawee Chiarawipa[1,*], Monsuang Rueangkhanab[2], Zhen Hai Han[3]

[1]*Agricultural Innovation and Management Division, Faculty of Natural Resources, Prince of Songkla University, Songkhla 90112, Thailand*
[2]*Office of Agricultural Research and Development Region 8, Department of Agriculture, Ministry of Agriculture and Cooperatives, Songkhla 90110, Thailand*
[3]*Institute for Horticultural Plants, College of Agronomy and Biotechnology, China Agricultural University, Beijing 100193, China*

Received 23 August 2020; Received in revised form 15 November 2020
Accepted 16 December 2020; Available online 6 September 2021

ABSTRACT

Leaf aging induces various photosynthetic responses through changes in the growth and development of vines. This study aimed to estimate the responses of leaf photosynthetic capacity and leaf nitrogen content (*N*) investments throughout the growing season. The altered ambient light intensity and CO_2 concentrations were demonstrated to affect the leaf photosynthetic capacity in grapevines at three different years of age based on non-rectangular hyperbola and A/C_i model approaches. The leaf growth stages were significantly higher for all leaf photosynthetic parameters than for the vine age factor, as estimated from the two main model approaches. In addition, the acclimation of the light-saturated photosynthetic rate (P_{max}), maximum carbon assimilation rate (A_{max}), apparent maximum rate of carboxylation due to Rubisco activity ($V_{c,max}$) and apparent maximum rate of electron transport in RuBP regeneration (J_{max}) showed slight differences among vine ages, which gradually increased starting at 4 weeks and suddenly declined during the senescence stage, at 20 weeks after leaf unfolding. Similarly, the leaf *N* investments in terms of the photosynthetic nitrogen use efficiency (*PNUE*), Rubisco (P_r), bioenergetics (P_b) and thylakoid light harvesting (P_l) were slightly higher in the 18-year-old vines than the other vines. There was a stronger relationship between *N* investments and $V_{c,max}$ than J_{max} when the data for all leaf growth stages and vine ages were pooled. These findings suggest that this variation may lead to differences in the potential to predict photosynthetic carbon gains among leaves and vines of different ages.

***Corresponding author:** rawee.c@psu.ac.th

Keywords: Carbon assimilation; Leaf structural traits; Photosynthesis model; Photosynthetic nitrogen use efficiency; Seasonal changes

1. Introduction

Photosynthetic carbon assimilation results directly from the photosynthetic reaction before carbon is translocated for accumulation or storage in the living parts of plants [1]. Among leaf development stages, the leaf becomes the main carbon absorption source in plants, which plays an important role in determining the fixation of CO_2 for growth and biomass production throughout the growing season [2].

Photosynthesis models have become an important tool that have been used widely for analysis of the photosynthetic responses of plant leaves [3]. Due to the acclimation of photosynthesis to light, it can be described based on a non-rectangular hyperbola (*NRH*) model as a steady state response to leaf irradiance [4-5]. Furthermore, biochemical models based on determining CO_2 concentration rates under different leaf temperature conditions are frequently analyzed with respect to the maximum carboxylation rate ($V_{c,max}$) [6], the maximum rate of electron transport (J_{max}) and triose-phosphate utilization (*TPU*), which were originally considered to be the three rate limiting steps in C_3 plants and were subsequently developed for considering photosynthetic responses, as mathematically expressed by [7-8] using the following parameters: 1) the RuBP-saturated rate of CO_2 assimilation (Rubisco-limited rate), 2) the RuBP-limited rate of CO_2 assimilation (electron transport-limited rate) and 3) the export-limited rate of CO_2 assimilation (phosphate-limited rate).

In addition to the changes that occur in photosynthetic responses based on several environmental factors, photosynthetic activities are also strongly limited by leaf ontogeny [9], leaf age [10] or other leaf structural traits [11]. Photosynthetic behaviors as a function of leaf age are usually related to the leaf nitrogen distribution [12-13], particularly resulting from acclimation to seasonal variability and leaf structural traits [14]. The leaf age-related effect on the seasonal/nitrogen relationship is closely linked to the leaf nitrogen use efficiency [15], which is expressed as the maximum carbon assimilation rate (A_{max}) per unit of leaf nitrogen/area (N_a) or on the basis of a leaf nitrogen/mass unit (N_m) over the growing season. In this relationship, the variation in the photosynthetic nitrogen use efficiency (*PNUE*) has been used to consider acquisition and assimilation over the leaf life span [16]. Moreover, $V_{c,max}$ and J_{max} are the main parameters used for considering photosynthetic functions based on the nitrogen fractions allocated to Rubisco (P_r) and to bioenergetics (P_b) [17].

The indeterminate growth habit of grapevines is primarily governed by leaf ontogeny and leaf age over the course of the growing season. The different leaf ages within a canopy can be ascribed to changes in the intercepted light [18] or temperature acclimation [19] by leaf photosynthetic responses. Additionally, the chlorophyll content, Rubisco activity, photosynthetic electron transport activities and thylakoid proteins in the grape leaf are strongly associated with the process of leaf aging [20]. Light-harvesting complexes of thylakoid proteins are responsible for transporting light energy, which is essentially invested in carbon assimilation [21]. It is therefore likely that the acclimation of the photosynthetic capacity, which results in changes in leaf ages, can be used for predicting the carbon gain potential associated with the leaf life span.

The aim of this study was to estimate the acclimation of the photosynthetic capacity and nitrogen partitioning to the photosynthetic apparatus in leaves and vines of different ages during the growing season.

Two main modeling approaches (*NRH* and biochemical models) were used for the estimation of photosynthetic functions, including some leaf structural traits, for calculating the *N* investment fractions.

2. Materials and Methods

2.1 Experimental site and plant material

The experiment was conducted in the Daxing district (39°73'N, 116°33'E) in northern China (Beijing region) during the growing season (April-September). A commercial hybrid grapevine cultivar (*Vitis vinifera* L. *x Vitis labrusca* L. 'Kyoho') was used as the experimental plant material; plants were spaced at 3.00 × 0.70 m (≈4,000 vines/ha) and grown on Y-shape trellises in a commercial vineyard.

Three healthy grapevines of each vine age (5-, 10- and 18-years) were used in the experiments. Leaf measurements were performed at 5 time points: 4, 8, 12, 16 and 20 weeks after leaf unfolding, according to the beginning of the main phenological events occurring after leaf unfolding. The timing of these events were as follows: anthesis or blooming stage (5th week), véraison stage (10th week) and harvesting stage (18th week). For all of the sampled vines, leaves of the same age that were fully exposed to the sun were selected and marked with plastic tags. Three leaves of a similar age per vine were randomly measured to determine gas exchange parameters. Subsequently, three leaves at the same stages were collected and used as three replicates, and these data were averaged to analyze photosynthetic activity according to the leaf area, leaf dry mass and chlorophyll and nitrogen content.

2.2 Leaf photosynthetic parameters

Leaf photosynthetic responses were analyzed in field trial conditions with a portable photosynthesis system (LI-6400XT, Li-Cor Inc., Lincoln NE, USA). For the first experiment addressing leaf photosynthetic parameters, quantitative responses associated with leaf photosynthesis were obtained for the light- saturated photosynthetic rate (P_{max}), apparent quantum yield, or photosynthetic efficiency (ϕ), light curve convexity (Θ), dark respiration (R_d), light saturation index (I_s) and light compensation index (I_c) [22], which were considered by fitting based on a non-rectangular hyperbola (*NRH*) model. The net photosynthesis rate (P_n) could then be calculated using the following Eq. (2.1) [4-5]:

$$P_n = \frac{\phi.I + P_{max} - \sqrt{\left((\phi.I + P_{max})^2 - 4\Theta.\phi.I.P_{max}\right)}}{2\Theta} - R_d. \quad (2.1)$$

Photosynthetic curves were determined under an altered ambient LED light source (6400-02B) at intervals of 200 μmol m^{-2} s^{-1}, up to 2,000 μmol m^{-2} s^{-1}. The ambient CO_2 concentration and leaf chamber temperature were constantly controlled at 400 μmol CO_2 mol^{-1} and 25 °C, respectively.

The second experiment examining leaf photosynthetic parameters involved examination of the apparent maximum rate of carboxylation due to Rubisco activity ($V_{c,max}$), the apparent maximum rate of electron transport in RuBP regeneration (J_{max}) and triose-phosphate utilization (*TPU*) using the photosynthesis models of [6], as applied by [23], with Eqs. (2.2), (2.3) and (2.4):

$$W_c = \frac{V_{c,max}.C_i}{C_i + K_c(1 + O/K_o)}, \quad (2.2)$$

$$J_{max,c} = \frac{(A_{max} + R_d)(4.5C_i + 10.5\Gamma^*)}{(C_i - \Gamma^*)}, \quad (2.3)$$

$$W_p = 3.V_{TPU}. \quad (2.4)$$

Here, W_c is the potential rate of CO_2 assimilation due to Rubisco activity; C_i is the intercellular partial pressure of CO_2; O is the oxygen concentration; K_c and K_o are the Michaelis-Menten constants of Rubisco activity for carboxylation and oxidation,

respectively; A_{max} is the maximum carbon assimilation rate μmol CO_2 m^{-2} s^{-1}); and Γ^* is the CO_2 compensation point. Finally, the phosphate- limited photosynthesis rate (W_p) which is limited at high CO_2 concentration levels, can be estimated from the velocity of *TPU* (V_{TPU}). To estimate the values of $V_{c,max}$, J_{max}, *TPU* and R_d, linear curve fitting was used from the Rubisco and RuBP- limited portion of the A/C_i response curves, as described by [24]. Additionally, in the present study, J_{max} can be estimated using Eq. (2.3) and then expressed as $J_{max,c}$, which is obtained from gas exchange measurements and is strongly related to the other described method [25]. The A/C_i response was determined continuously using a leaf chamber at 25 °C under a photosynthetic photon flux density (PPFD) of 1,200 μmol $m^{-2}s^{-1}$ and a relative humidity of 40-50%. The CO_2 concentration was regulated, beginning at 400, 200, 100, 75, 50, 25 or 0 μmol CO_2 mol^{-1}, followed by 370, 600, 800, 1,000, 1,200, 1,500 or 1,800 μmol CO_2 mol^{-1}, respectively. Most of the gas exchange parameters were only measured during the period of 09:00-15:00 on clear days. Additionally, the carbon assimilation rate (A) and the parameters C_i, C_c (CO_2 concentration at the site of Rubisco at the chloroplast level) and Γ^* were also determined for measurement of the mesophyll conductance (g_m) in the leaves as required parameters for curve fitting using modeling method (Eq. (2.5)) [26]:

$$g_m = \frac{A}{C_i - C_c}. \quad (2.5)$$

2.3 Leaf structural traits in the photosynthetic apparatus

2.3.1 Leaf chlorophyll content

Each leaf was cut into two 1 mg samples from the middle portion of the leaf blade and extracted with *N,N*-dimethylformamide (DMF) to determine the total chlorophyll content (*Chl*) (mg L^{-1}). The absorption of each chlorophyll sample was recorded at 647 and 664 nm with a UV spectrophotometer (UV-2550, Shimadzu, Tokyo, Japan) and the total *Chl* was quantified with the equations described by [27].

2.3.2 Leaf nitrogen content

The individual leaf area was measured using an LI-3000C portable leaf area meter (Li-Cor Inc., Lincoln NE, USA). The sampled leaves were harvested directly and dried in an oven at 65 °C for 48 hours, and the leaf dry mass was then measured to determine the leaf mass per unit area (*LMA*). Finely ground tissues were digested to determine the total leaf nitrogen content (N) using the Kjeldahl method. Based on nitrogen partitioning to the photosynthetic apparatus, the apparent fractions of N per unit of leaf area (N_a) and leaf dry mass (N_m) were used and expressed on a basis of either mass or area for determining leaf structural traits. In addition, the N investment fractions could be used to perform estimations in terms of the *PNUE* (N allocated to A_{max}), Rubisco (P_r) (Eq. (2.6)), bioenergetics (P_b) (Eq. (2.7)) and thylakoid light harvesting (P_l) (Eq. (2.8)) according to [21] and represented by [28], which were calculated as follows:

$$P_r = \frac{V_{c,max}}{(6.25 \text{x} V_{cr} \text{x} N_a)}, \quad (2.6)$$

$$P_b = \frac{J_{max}}{(8.06 \text{x} J_{mc} \text{x} N_a)}, \quad (2.7)$$

$$P_l = \frac{Cc}{(N_m \text{x} C_B)}, \quad (2.8)$$

where V_{cr} and J_{mc} are the maximum rate of RuBP carboxylation (mol CO_2 g^{-1} Rubisco s^{-1}) and the photosynthetic electron transport capacity (mol e^- mol cyt f^{1} s^{-1}) at a leaf temperature of 25 °C, respectively; *Cc* is the leaf chlorophyll concentration (mmol g^{-1}), and C_B is the constant of chlorophyll binding of the thylakoid protein complexes (mmol *Chl* (g N)$^{-1}$), as calculated and described by

[21, 29]; the values of J_{max} are obtained from $J_{max,c}$ as described above.

2.4 Statistical analyses

Statistical analyses were conducted using SPSS 15.0 (SPSS Inc., Chicago, USA). The data were subjected to two-way analysis of variance (ANOVA) to compare the effects of leaf developmental stages and vine ages for all of the measured parameters. Statistically significant differences in means were compared using Tukey's HSD (honestly significant difference) test. The relationships between the apparent nitrogen investment fractions and photosynthetic parameters were tested using Pearson's correlation and simple linear regression procedures to examine significance.

3. Results and Discussion

3.1 Changes in leaf photosynthetic parameters under light-saturating and biochemical limitations

The differences in the leaf growth stage responses are presented in Fig. 1. P_{max} increased sharply from 4 to 12 weeks and remained stable from 12 to 16 weeks, then gradually declined again until senescence occurred at 20 weeks. In contrast, the maximum value was reached at 8 weeks in 5-year-old vines. Conversely, R_d decreased dramatically at 8 weeks and remained stable until 16 weeks, before slowly increasing again at 20 weeks. I_c, which showed a pattern similar to R_d in all vines across each leaf growth stage, decreased rapidly after the first stage and then increased slightly in the last stage. In addition, there was evidence of I_s in the acclimation response. Although this index was slightly higher in 5-year-old vines at 4 weeks after leaf unfolding, the I_s values fluctuated between 700 and 1,000 μmol m^{-2} s^{-1} in each leaf growth stage.

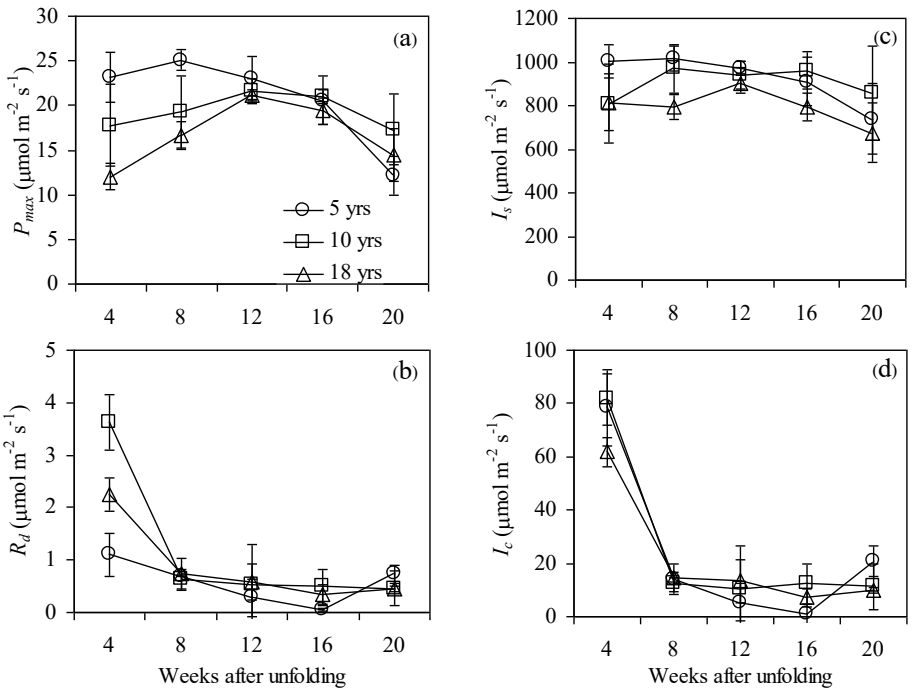

Fig. 1. Changes in the light-saturated photosynthetic rate (P_{max}) (a), dark respiration rate (R_d) (b), light saturation index (I_s) (c) and light compensation index (I_c) (d) in grape leaves at 4, 8, 12, 16 and 20 weeks after unfolding on grapevines of different ages (bars represent mean ± sd, n= 3).

Fig. 2 shows the pattern of A/C_i responses during the five leaf growth stages in the vines of three different ages during the growing season. A_{max} showed the same pattern as $V_{c,max}$, J_{max} and TPU throughout the period of leaf development. The highest values of these parameters were achieved at 8 to 16 weeks, after increasing at the beginning, and then steadily declining at the end of the leaf growth stages, though this pattern differed for R_d, which was similar to the results of the *NRH* model. The steady decline in R_d began at 4 weeks and lasted until 16 weeks; a slight increase was then observed at 20 weeks, especially in 10-year-old vines, while R_d for both 5- and 18-year-old vines remained fairly stable at 16 and 20 weeks. Despite the large differences in g_m detected in the early stage for all vine ages, g_m reached its peak at around 12 weeks and decreased gradually during the last stage.

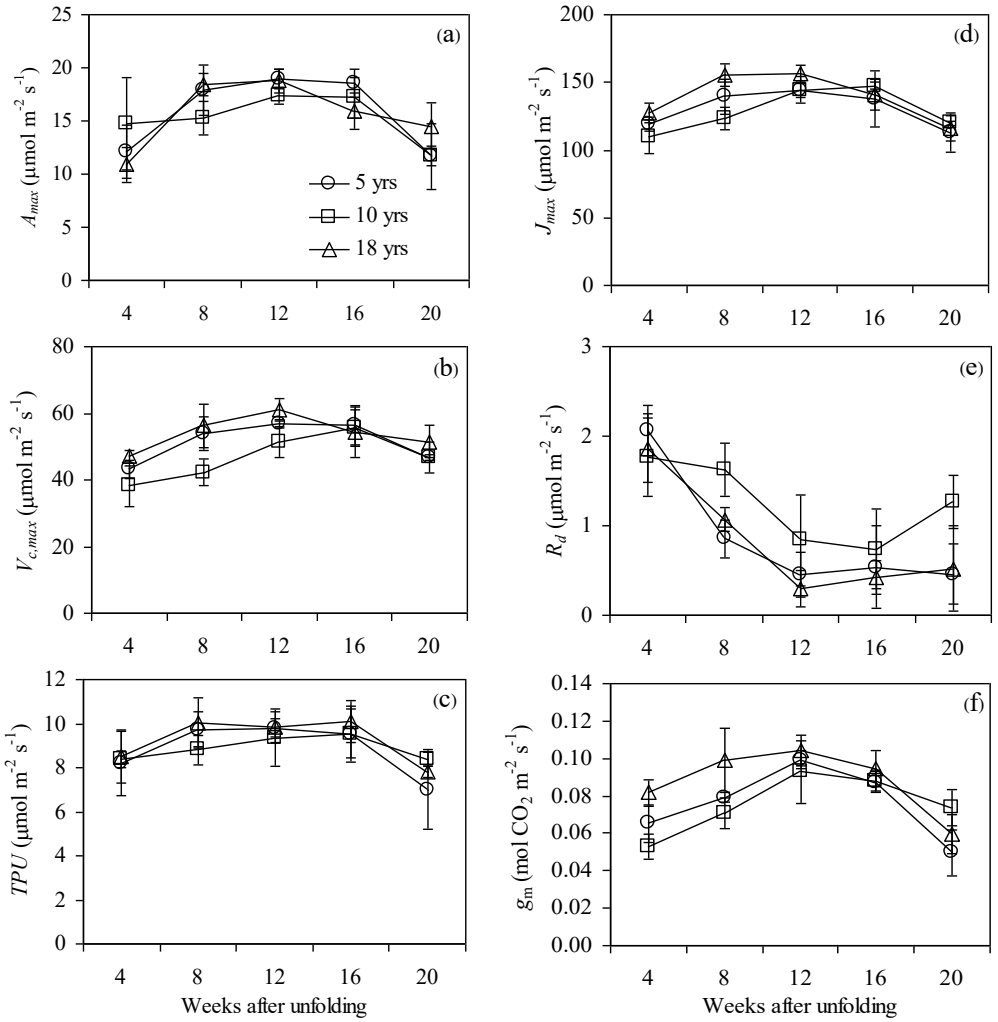

Fig. 2. Changes in the maximum carbon assimilation rate (A_{max}) (a), apparent maximum rate of carboxylation ($V_{c,max}$) (b), triose-phosphate utilization (TPU) (c), apparent maximum rate of electron transport (J_{max}) (d), dark respiration rate (R_d) (e) and mesophyll conductance (g_m) (f) in grape leaves at 4, 8, 12, 16 and 20 weeks after unfolding on grapevines of different ages (bars represent mean ± sd, n= 3).

3.1.1 Photosynthetic capacity in different ages of grapevine leaves

There was evidence for an effect of the leaf growth stage on the photosynthetic capacity under light-saturating conditions, as estimated using the *NRH* model. The acclimation patterns of P_{max} and I_s appeared to be dependent upon leaf and vine ages (Fig. 1). This pattern was similar regarding the seasonal variability during the growing season (April-September) in photosynthetic parameters and leaf ages, which have commonly shown higher values in either fully expanded leaves or mature stages and decrease thereafter during the senescence stage in *V. vinifera* L. 'Pinot noir' [20] and *V. vinifera* L. 'Syrah' leaves [30]. This may be due to the fact that young leaves are not completely developed for performing photosynthetic assimilation, which then declines during the acceleration of the senescence phenomenon in the leaf [31]. In contrast, R_d showed a peak incidence in young leaves and then decreased with leaf age. Vine leaves show a high response rate regarding the partitioning of respiration into its growth and maintenance components in the early stage of leaf growth, while a lower rate of maintenance respiration is dominant in older leaf stages [32]. During leaf maturation and senescence, it has been suggested that the decrease in respiration might be caused by a low availability of solutes, due to their translocation to other parts of the vine; this translocation of solutes out from leaves in the dark requires energy gained from respiration [33].

Furthermore, a decline in I_c is likely to be imposed by changes in the respiration processes in response to different leaf ages, as observed in both *V. vinifera* L. 'Riesling' and 'Chasselas' [34]. In addition, these photosynthetic parameters were also affected by changes in vine age-related acclimation, despite the fact that the highest mean values of P_{max} and R_d were observed in 10- and 5-year-old vines, respectively. It is possible that the photosynthetic capacity varies under age-related changes in vines of different ages. In this regard, photosynthetic responses have also been observed in other woody plants, although these changes were not found to be greater in the oldest trees as compared to both the juvenile and mature trees [35].

The leaves from vines of all three ages showed a similar pattern regarding their photosynthetic capacity under the investigated CO_2 concentration conditions, as estimated by the A/C_i curve-fitting method (Fig. 2). It is notable that the acclimation of the photosynthetic capacity of the leaves was predominantly determined by the leaf growth stage, as evidenced by the high significance of all investigated parameters found for the leaf age factor. In contrast, the trends in $V_{c,max}$, J_{max}, TPU and A_{max} were similar between different vine ages. Therefore, it is possible to estimate the changes in biochemical limitations, especially for $V_{c,max}$ and J_{max}, as a strong relationship was observed between leaf age-dependent variation and A_{max} [36].

Although the photosynthetic capacity increased with leaf age during development and declined thereafter, the variations in this capacity were strongly linked to the change in g_m [37], as a higher g_m was recorded at 8 to 16 weeks. This association is mainly due to the fact that the leaf growth stage is strongly limited by the response of g_m to intercellular CO_2 concentrations, imposing a constant degree of limitation on the leaf photosynthetic capacity [38], especially for $V_{c,max}$ and J_{max}, which were significantly lower in both young and senescing leaves than leaves in other growth stages. In addition, it has previously been found that an increasing demand for CO_2 is associated with a higher g_m response, leading to an increased CO_2 concentration in chloroplasts [39]. Therefore, g_m can be directly affected by the number of chloroplasts, which varies with structural traits in leaves of different ages [11]. The results of this study imply that vine leaves in the mature stage, or at 8 to 16 weeks

of age, possess a greater potential ability to fix carbon than both young and senescing leaves.

3.2 Changes in the apparent *N* investment fractions and the photosynthetic apparatus

The results regarding leaf nitrogen partitioning to photosynthetic apparatus are shown in Fig. 3. Despite the differences detected between the vine ages regarding the leaf mass per unit area (*LMA*) in the different leaf growth stages, slightly higher values were found when the leaves were undergoing senescence than in earlier stages. In contrast, the values of N_m decreased from the beginning to the last leaf growth stages. The values of N_a were found to show almost the same pattern as N_m in all leaf growth stages, being significantly lower in 18-year-old vines than in the other two vine ages, with the exception of the 12-week stage. Differences in total *Chl* were also found between different leaf and vine ages. The total *Chl* contents for all leaves were highest at 16 weeks before declining dramatically at 20 weeks.

Leaf *N* and total *Chl* responded in a similar manner to photosynthetic functions both between different leaf growth stages and different vine ages. The *PNUE* values for both 5- and 10-year-old vines increased significantly from 4 to 12 or 16 weeks, but remained stable from 12 to 20 weeks for 18-year-old vines. The value of P_r was slightly higher for 18-year-old vines and was lowest for 10-year-old vines. The results for 18-year-old grapevines were highly similar to those for 10-year-old vines, steadily increasing until 20 weeks, whereas the values suddenly decreased for both 5- and 10-year-old vines. In addition, P_b was highest in 18-year-old vines at all leaf growth stages, except for at 12 weeks, when P_b values were similar to the other two vine ages, and the values for all sampling stages decreased at 20 weeks. There were no large differences in P_l detected between the three vine ages, which seemed to favor 18-year-old vines over either 5- or 10-year-old vines, especially in the 16-20-week leaf growth stages. However, there was a reduction in P_l at the last stage, which followed a similar pattern as previously shown for P_b. Fitting the linear relationships between the apparent fraction of *N* investments to $V_{c,max}$ and to J_{max} resulted in a high coefficient of determination (r^2) associated with significant differences for the pooled data for all leaf growth stages and vine ages (Fig. 4). There were positive correlations observed for both $V_{c,max}$ and J_{max}, although the highest r^2 values were found for $V_{c,max}$ with all of the *N* investment parameters. Regarding *PNUE* activity, it was significantly different for $V_{c,max}$ ($P \leq 0.01$) and slightly lower for J_{max} ($P \leq 0.01$). Highly significantly differences were found in $V_{c,max}$ for both P_r and P_b, though the difference decreased significantly for J_{max}. However, the lowest significant differences were found in P_l for both $V_{c,max}$ and J_{max} ($P \leq 0.05$).

3.2.1 Photosynthetic nitrogen use efficiency in different ages of grapevine leaves

The pattern of changes in the leaf photosynthetic capacity was found to be almost the same as the pattern of changes in leaf structural traits, in which an increased leaf mass was associated with increases in *LMA* and total *Chl* in vines of all three ages (Fig. 3). On the basis of the leaf mass and leaf area, *LMA* and total *Chl* were high as the leaves rapidly expanded during spring and slightly declined at the end of the growing season. The apparent *N* fractions declined with increasing leaf age when expressed on a mass or an area basis for N_m and N_a, respectively. Thus, there was a high demand for *N* for contributing to new vine leaf growth in early stages, though a decrease might occur during leaf ontogeny, especially if either leaf mass or leaf area is not a limitation for the growth distribution over the growing season [9, 40].

In the same leaf growth stages, *PNUE*, P_r, P_b and P_l were strongly influenced by the acclimation of leaf *Chl* and leaf *N* per unit of leaf area and leaf mass, regardless of the environmental conditions. A similar pattern was observed during the growing season in olive trees [38], where a higher leaf *N* content in terms of both N_m and N_a likely enhanced the photosynthetic capacity. Moreover, the variations in P_r and P_b, which are derived from both photosynthetic functions ($V_{c,max}$ and J_{max}), were specifically impacted by N_a, as previously reported for woody plants [28]. Despite the dependence of N_m on light-harvesting components (P_l), the capacity for light utilization was remarkably similar to the total *Chl* content in vines of different ages. This is mainly due to the fact that leaf *Chl* is associated with soluble proteins in the thylakoid membranes of chloroplasts, which decline during the senescence stage of grape leaves [41]. The degradation of these proteins may result in an altered photosynthetic capacity during the senescence stage in the vines of all three ages.

Additionally, soluble proteins have been found to show a linear relationship to N_m under growth irradiance and to directly affect photosystem I (PSI) and photosystem II (PSII), including the light-harvesting chlorophyll protein complexes of the chloroplast thylakoid involved in photosynthetic electron transport [29]. Consequently, changes in the proportions of *N* and total *Chl* could reflect the photosynthetic light harvesting capacity of C_3 plants [12]. Thus, the quantitative partitioning of both leaf *N* and total *Chl* can play a significant role in determining the light harvesting efficiency of vine leaves with regard to the carbon gain potential associated with the acclimation of leaf structural traits during seasonal changes, although light harvesting efficiency might be tightly restricted by environmental light conditions [21] and *N* supply [42] for leaf photosynthesis. Coincidently, the results obtained regarding the relationships between the key parameters of photosynthetic capacity ($V_{c,max}$ and J_{max}) and *N* investments in the photosynthetic machinery showed that they followed changes in leaf structural traits, total *Chl* and leaf *N* partitioning among the periods of the growing season. The r^2 results (Fig. 4) show that the proportion of *N* might be more highly invested in carboxylation functions than in electron transport functions, which is consistent with the positive relationship between $V_{c,max}$ and the fractional leaf nitrogen investment, or between A_{max} and *N* associated with Rubisco activity [43] based on age-related changes in leaf structural traits. Furthermore, it appears likely that the function of Rubisco in the storage of *N* preserved changes in the balance between the carboxylation capacity and electron transport capacity in addition to its catalytic role [44].

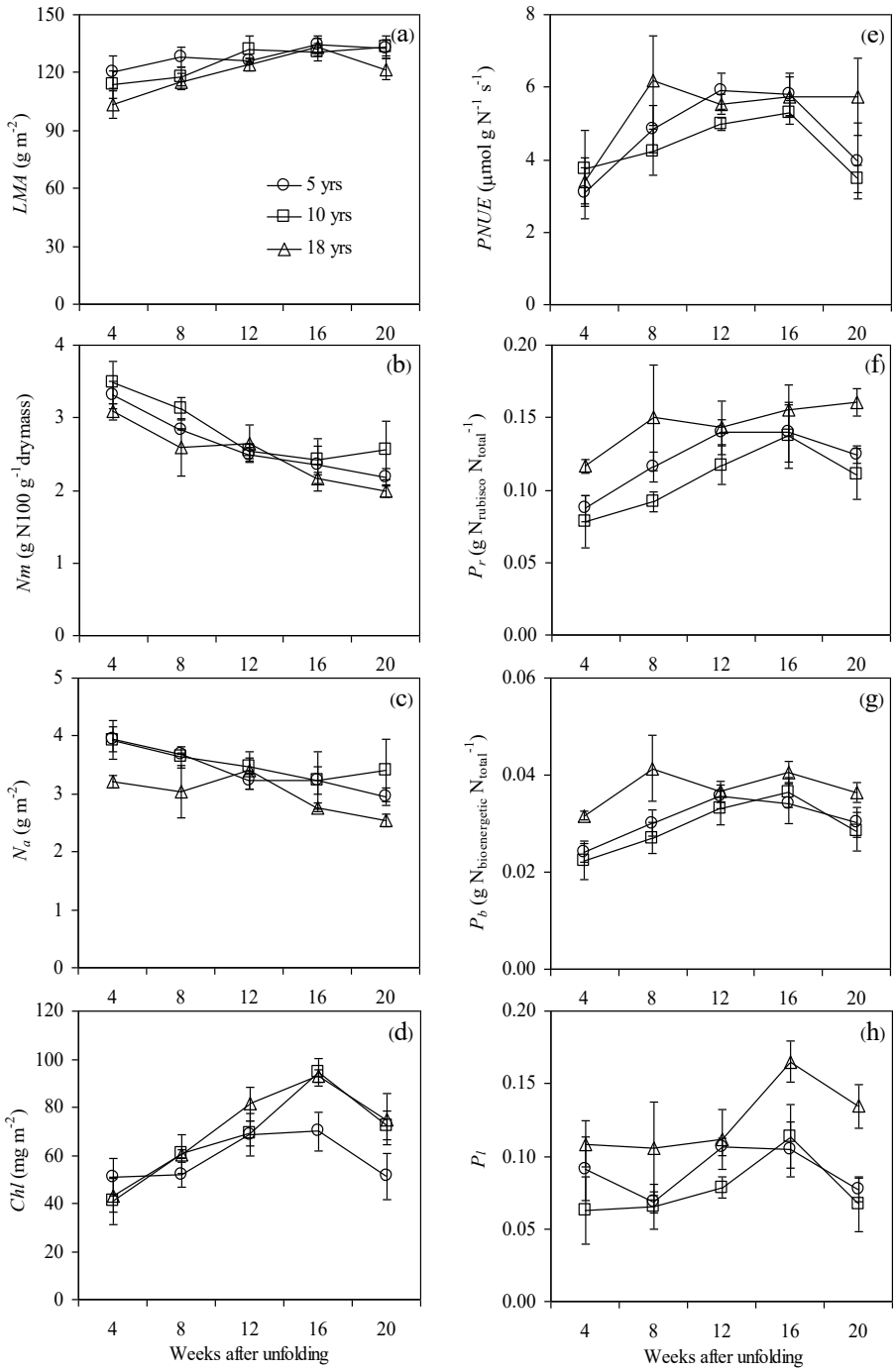

Fig. 3. Changes in the leaf mass per unit area (*LMA*) (a), fraction of *N* in the leaf dry mass (N_m) (b), amount of *N* per unit of leaf area (N_a) (c), total chlorophyll content (*Chl*) (d), *N* allocated to A_{max} (*PNUE*) (e), *N* allocated to Rubisco (P_r) (f), *N* allocated to bioenergetics (P_b) (g) and *N* allocated to thylakoid light harvesting (P_l) (h) in grape leaves at 4, 8, 12, 16 and 20 weeks after unfolding in different ages of grapevines (bars represent mean ± sd, n= 3)

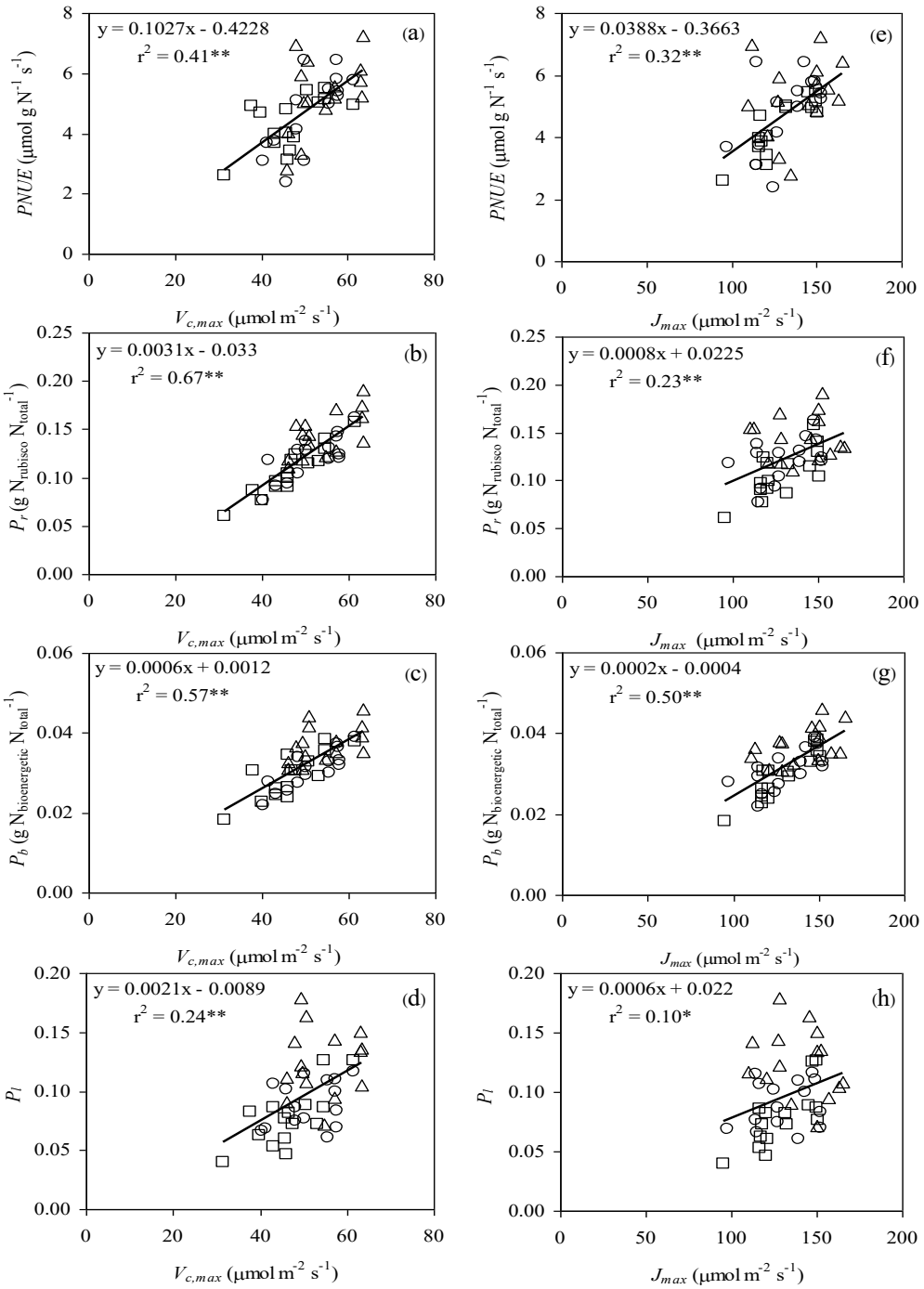

Fig. 4. The linear relationships between the apparent maximum rate of carboxylation ($V_{c,max}$) (a-d) and the apparent maximum rate of electron transport (J_{max}) (e-h) with the fractions of *N* allocated to A_{max} (*PNUE*) (a,e), *N* allocated to Rubisco (P_r) (b,f), *N* allocated to bioenergetics (P_b) (c,g) and *N* allocated to thylakoid light harvesting (P_l) (d,h) in grape leaves at 4, 8, 12, 16 and 20 weeks after unfolding on grapevines of different ages (asterisks (*,**) represent a significant effect (P≤0.05 or P≤0.01) according to the Tukey's HSD test)

4. Conclusion

This study showed that photosynthetic functions were related to the acclimation occurring across vine ages, even though they were only slightly affected by some aspects of photosynthetic parameters. Leaf age seemed to be a more impactful factor than vine age, as demonstrated by the leaf photosynthetic responses that occurred throughout the growing season. Therefore, it can be concluded that the acclimation of structural traits and the partitioning of total *Chl* and *N* in grape leaves were directly induced by age-related phenomena. All of the *N* allocation to photosynthetic functions (*PNUE,* P_r, P_b and P_l) is specifically imposed by the leaf *N* acquisition activity and photosynthetic capacity potential. The age-related changes in the functional investment of *N* might therefore mainly limit the carbon gain in grape leaves. Finally, the age-related acclimation of the net carbon gain per unit leaf area needs to be considered in further studies to assess carbon sequestration during the growing season, particularly in grapevines of different ages.

Acknowledgements

Financial support and grants from the earmarked fund for China Agriculture Research System (CARS-28), special fund for Agro- scientific Research in the Public Interest (201203075), and Ministry of Agriculture Key Laboratory of Biology and Genetic Improvement of Horticultural Crops (Nutrition and Physiology) are gratefully acknowledged. The authors are also very thankful to anonymous reviewers for their greatly constructive comments.

References

[1] Lambers H, Chapin III FS, Pons TL. Plant Physiological Ecology, 2nd ed. New York: Springer; 2008.

[2] Chytyk CJ, Hucl PJ, Gray GR. Leaf photosynthetic properties and biomass accumulation of selected western Canadian spring wheat cultivars. Can J Plant Sci 2011;91:305-14.

[3] Farquhar GD, von Caemmerer S, Berry JA. Models of photosynthesis. Plant Physiol 2001;125: 42-5.

[4] Ögren E, Evans JR. Photosynthetic light-response curves. Planta 1993;189:182-90.

[5] Thornley JHM. Dynamic model of leaf photosynthesis with acclimation to light and nitrogen. Ann Botany 1998;81: 421-30.

[6] von Caemmerer S, Farquhar GD. Some relationships between the biochemistry of photosynthesis and the gas exchange of leaves. Planta 1981;153:376-87.

[7] Farquhar GD, von Caemmerer S, Berry JA. A biochemical model of photosynthetic CO_2 assimilation in leaves of C_3 species. Planta 1980;149:78-90.

[8] von Caemmerer S. Biochemical Models of Leaf Photosynthesis. Victoria: CSIRO Publishing; 2000.

[9] Oleksyn J, Zytkowiak R, Reich PB, Tjoelker MG, Karolewski P. Ontogenetic patterns of leaf CO_2 exchange, morphology and chemistry in *Betula pendula* trees. Trees 2000;14:271-81.

[10] Kitajima K, Mulkey SS, Samaniego M, Wright SJ. Decline of photosynthetic capacity with leaf age and position in two tropical pioneer tree species. Am J Bot 2002;89:1925-32.

[11] Niinemets Ü, Cescatti A, Rodeghiero M, Tosens T. Leaf internal diffusion conductance limits photosynthesis more strongly in older leaves of Mediterranean evergreen broad-leaved species. Plant Cell Environ 2005;28:1552-66.

[12] Evans JR. Photosynthesis and nitrogen relationships in leaves of C_3 plants. Oecologia 1989;78:9-19.

[13] Thornley JHM. Acclimation of photosynthesis to light and canopy nitrogen distribution: An interpretation. Ann Botany 2004;93:473-5.

[14] Yasumura Y, Hikosaka K, Hirose T. Seasonal changes in photosynthesis, nitrogen content and nitrogen partitioning in *Lindera umbellata* leaves grown in high or low irradiance. Tree Physiol 2006;26:1315-23.

[15] Egea G, González-Real MM, Baille A, Nortes PA, Conesa MR, Ruiz-Salleres I. Effects of water stress on irradiance acclimation of leaf traits in almond trees. Tree Physiol 2012;32:450-63.

[16] Feng YL. Nitrogen allocation and partitioning in invasive and native *Eupatorium* species. Physiol Plant 2008;132:350-8.

[17] Chang W, Zhang SB, Li SY, Hu H. Ecophysiological significance of leaf traits in *Cypripedium* and *Paphiopedilum*. Physiol Plant 2011;141:30-9.

[18] Palliotti A, Cartechini A, Ferranti F. Morpho- anatomical and physiological characteristics of primary and lateral shoot leaves of Cabernet Franc and Trebbiano Toscano grapevines under two irradiance regimes. Am J Enol Vitic 2000;51:122-30.

[19] Hendrickson L, Ball MC, Wood JT, Chow WS, Furbank RT. Low temperature effects on photosynthesis and growth of grapevine. Plant Cell Environ 2004;27:795-809.

[20] Bertamini M, Nedunchezhian N. Leaf age effects on chlorophyll, Rubisco, photosynthetic electron transport activities and thylakoid membrane protein in field grown grapevine leaves. J Plant Physiol 2002;159:799-803.

[21] Niinemets Ü, Tenhunen JD. A model separating leaf structural and physiological effects on carbon gain along light gradients for the shade-tolerant species *Acer saccharum*. Plant Cell Environ 1997;20:845-66.

[22] Johnson IR, Parsons AJ, Ludlow MM. Modelling photosynthesis in monocultures and mixtures. Aust J Plant Physiol 1989;16:501-16.

[23] Long SP, Bernacchi CJ. Gas exchange measurements, what can they tell us about the underlying limitations to photosynthesis? Procedures and sources of error. J Exp Bot 2003;54:2393-401.

[24] Pimentel C, Bernacchi C, Long S. Limitations to photosynthesis at different temperatures in the leaves of *Citrus limon*. Braz J Plant Physiol 2007;19:141-7.

[25] Bernacchi CJ, Pimentel C, Long SP. *In vivo* temperature response functions of parameters required to model RuBP-limited photosynthesis. Plant Cell Environ 2003;26:1419-30.

[26] Harley PC, Loreto F, Marco GD, Sharkey TD. Theoretical considerations when estimating the mesophyll conductance to CO_2 flux by analysis of the response of photosynthesis to CO_2. Plant Physiol 1992;98:1429-36.

[27] Inskeep WP, Bloom PR. Extinction coefficients of chlorophyll *a* and *b* in *N,N*-Dimethylformamide and 80% Acetone. Plant Physiol 1985;77:483-5.

[28] Delagrange S. Light- and seasonal-induced plasticity in leaf morphology, N partitioning and photosynthetic capacity of two temperate deciduous species. Environ Exp Bot 2011;70:1-10.

[29] Niinemets Ü, Kull O, Tenhunen JD. An analysis of light effects on foliar morphology, physiology, and light interception in temperate deciduous woody species of contrasting shade tolerance. Tree Physiol 1998;18:681-96.

[30] Prieto JA, Giorgi EG, Peňa JP. Modelling photosynthetic- light response on Syrah

leaves with different exposure. Vitis 2010;49:145-6.

[31] Koukkari WL, Hobbs LC, Salisbury FB. Phase shift in leaf movements of *Xanthium* attributed to age and rhythm patterns. Plant Physiol 1992;98:1381-5.

[32] Salisbury FB, Ross CW. Plant Physiology, 4th ed. California: Wadsworth Publishing Co.;1991.

[33] Bunce JA. Direct and acclimatory responses of dark respiration and translocation to temperature. Ann Bot 2007;100:67-73.

[34] Zufferey V, Murisier F, Schultz H. A model analysis of the photosynthetic response of *Vitis vinifera* L. cvs. Riesling and Chasselas leaves in the field: I. Interaction of age, light and temperature. Vitis 2000;39:19-26.

[35] Greenwood MS, Ward MH, Day ME, Adams SA, Bond BJ. Age-related trends in red spruce foliar plasticity in relation to declining productivity. Tree Physiol 2008;28:225-32.

[36] Zhang S, Hu H, Li Z. Variation of photosynthetic capacity with leaf age in an alpine orchid, *Cypripedium flavum*. Acta Physiol Plant 2008;30:381-8.

[37] Hanba YT, Miyazawa SI, Kogami H, Terashima I. Effects of leaf age on internal CO_2 transfer conductance and photosynthesis in tree species having different types of shoot phenology. Aust J Plant Physiol 2001;28:1075-84.

[38] Diaz-Espejo A, Nicolas E, Fernandez JE. Seasonal evolution of diffusional limitations and photosynthetic capacity in olive under drought. Plant Cell Environ 2007;30:922-33.

[39] Düring H. Stomatal and mesophyll conductances control CO_2 transfer to chloroplasts in leaves of grapevine (*Vitis vinifera* L.). Vitis 2003;42:65-8.

[40] Sirijaroonwong U, Kiratiprayoon S, Diloksumpun S, Ruenrit P. Some morphological characteristics of *Eucalyptus camaldulensis* Dehn. clone A5 and clone D1, at the clonal plantation in Eastern Thailand. Science & Technology Asia 2017;22:23-34.

[41] Bertamini M, Nedunchezhian N. Photosynthetic functioning of individual grapevine leaves (*Vitis vinifera* L. cv. Pinot noir) during ontogeny in the field. Vitis 2003;42:13-7.

[42] Pompelli MF, Martins SCV, Antunes WC, Chaves ARM, DaMatta FM. Photosynthesis and photoprotection in coffee leaves is affected by nitrogen and light availabilities in winter conditions. J Plant Physiol 2010;167:1052-60.

[43] Warren CR, Livingston NJ, Turpin DH. Photosynthetic responses and N allocation in Douglas-fir needles following a brief pulse of nutrients. Tree Physiol 2004;24:601-8.

[44] Warren CR, Dreyer E, Adams MA. Photosynthesis- Rubisco relationships in foliage of *Pinus sylvestris* in response to nitrogen supply and the proposed role of Rubisco and amino acids as nitrogen stores. Trees 2003;17:359-66.

Appendix

Abbreviations: A, carbon assimilation rate; A_{max}, maximum carbon assimilation rate; C_B, chlorophyll binding of the thylakoid protein complex; Cc, leaf chlorophyll concentration; C_c, CO_2 concentration in the chloroplast; Chl, chlorophyll content; C_i, intercellular partial pressure of CO_2; g_m, mesophyll conductance; I_c, light compensation index; I_s, light saturation index; J_{max}, apparent maximum rate of electron transport of RuBP regeneration; J_{mc}, capacity of photosynthetic electron transport; K_c, Michaelis-Menten constants of Rubisco activity for carboxylation; K_o, Michaelis-Menten constants of Rubisco activity for oxidation; LMA, leaf mass per unit area; N, nitrogen content; NRH, non rectangular hyperbola; N_a, fraction of N per unit of leaf area; N_m, fraction of N per unit of leaf dry mass; O, oxygen concentration; P_b, fraction of N

allocated to bioenergetics; P_{max}, light-saturated photosynthetic rate; P_l, fraction of N allocated to thylakoid light harvesting; P_n, net photosynthesis rate; *PNUE*, fraction of N allocated to A_{max}; *PPFD*, photosynthetic photon flux density; P_r, fraction of N allocated to Rubisco; R_d, dark respiration rate; *TPU*, triose-phosphate utilization; $V_{c,max}$, apparent maximum rate of carboxylation by Rubisco activity; V_{cr}, maximum rate of RuBP carboxylation; V_{TPU}, velocity of *TPU*; W_c, potential rates of CO_2 assimilation by Rubisco activity; W_p, phosphate-limited photosynthesis rate; ϕ, apparent quantum yield; Θ, light curve convexity; Γ^*, CO_2 compensation point.